

Cite this: *Dalton Trans.*, 2019, **48**, 4370Received 31st January 2019,  
Accepted 1st March 2019

DOI: 10.1039/c9dt00485h

rsc.li/dalton

## Salen supported Al–O–C≡P and Ga–P=C=O complexes†

Yanbo Mei,<sup>a</sup> Jaap E. Borger,<sup>b</sup> Dong-Jun Wu<sup>a,b</sup> and Hansjörg Grützmacher<sup>a,b</sup>

The first OCP adducts of aluminium and gallium are reported. The complexes are supported by sterically encumbered salen ligands and reveal a selective binding to O and P, respectively. Their reactivity with diazaphosphenium Lewis acids and N-heterocyclic carbene Lewis bases is described, in addition to cycloaddition reactions with s-tetrazines.

The development of versatile phosphorus building blocks allows new avenues to be explored in organophosphorus chemistry. A prominent example is the 2-phosphaethynolate anion, OCP<sup>-</sup>,<sup>1</sup> which represents the P-analogue of cyanate (OCN<sup>-</sup>) and can be prepared on multi-gram scale as sodium salt.<sup>2</sup> In recent years, its reactivity has been studied extensively revealing a plethora of transformations to be feasible leading to a broad spectrum of novel phosphorus compounds.<sup>3</sup> A prominent reaction step involves salt metathesis which leads to O- or, more frequently, to P-substituted products (Scheme 1). These facile syntheses of functionalized oxyphosphaalkynes (**A**) or phosphaketenes (**B**) allows the access to valuable starting materials which can be applied, for example, in P-heterocycle synthesis.<sup>3</sup>

Compounds of the type **A** can be generated in reactions of Na[OCP] with highly oxophilic s-block and actinide metal halide complexes (M = Ca,<sup>4</sup> Mg,<sup>5</sup> U,<sup>6,7</sup> Th<sup>6</sup>), as well as with those containing rare-earth metals (M = Sc,<sup>8</sup> Y,<sup>9</sup> Nd,<sup>9</sup> Sm<sup>9</sup>). Compounds of type **B** are more common and form when p-block element (E = P,<sup>10</sup> C,<sup>2b,11</sup> Ge,<sup>12</sup> Sn<sup>12a,13</sup>) or d-block metal (M = Re,<sup>14</sup> Co,<sup>15</sup> Ir,<sup>15</sup> Au,<sup>15</sup> Ti<sup>16</sup>) halide precursors are

employed.<sup>17,18</sup> In case of oxophilic organyl-substituted chlorosilanes<sup>13d,19</sup> or -boranes,<sup>20</sup> a mixture of both isomers **A** and **B** is obtained. The ratio is highly dependent on the reaction conditions. Notably, a diazaboryl chloride was recently reported to permit the synthesis of the first, and so far only, stable example of a main group element-coordinated phosphaethynolate adduct of the type **A**, that is (N(dipp)CH)<sub>2</sub>B–O–C≡P (dipp = 2,6-diisopropylphenyl).<sup>21,22</sup>

The coordination behaviour of Na[OCP] toward the heavier elements of the group 13 has not been studied to date, yet should provide further insight into the ambident nature of the phosphaethynolate salt and access to novel rare O-substituted compounds. Herein, the synthesis and isolation of the first OCP adducts of aluminium and gallium are reported. The complexes contain sterically encumbered salen ligands and revealed a selective binding preference to oxygen or phosphorus, respectively. The reactivity of the products toward Lewis acids and bases was probed, and their engagement in cycloaddition reactions with tetrazines assessed.

To start, commercially available diisobutylaluminum chloride (DIBAC) was reacted with Na[OCP] in C<sub>6</sub>D<sub>6</sub> at room temperature. The reaction produced a single species according to the multinuclear NMR spectra of the black mixture, with a singlet <sup>31</sup>P resonance signal at –331.5 ppm (see the ESI† for further details). *In situ* infrared spectroscopy revealed a strong absorption at  $\nu = 1676\text{ cm}^{-1}$ , which is indicative of O-bound phosphaethynolate complex **1** (Scheme 2). For comparison, the respective OCP stretching frequency in (N(dipp)CH)<sub>2</sub>B–O–C≡P is found in the same range at  $\nu = 1649\text{ cm}^{-1}$ ,<sup>21</sup> while that in Ph<sub>3</sub>Sn–P=C=O is located at  $\nu = 1946\text{ cm}^{-1}$ .<sup>13d</sup> Indeed, the

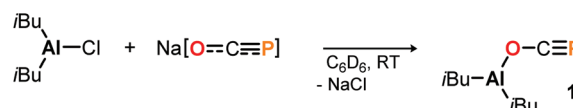


**Scheme 1** Generic salt metathesis reaction of Na[OCP] to give O- or P-substituted products.

<sup>a</sup>Department of Chemistry and Applied Biosciences, ETH Zürich, Vladimir-Prelog Weg 1, Hönggerberg, 8093 Zürich, Switzerland. E-mail: hgruetzmacher@ethz.ch, borger@inorg.chem.ethz.ch

<sup>b</sup>Lehn Institute of Functional Materials (LIFM), School of Chemistry, Sun Yat-sen University, 510275 Guangzhou, China

† Electronic supplementary information (ESI) available. CCDC 1860668, 1860669, 1860673, 1860732, 1860759 and 1876471. For ESI and crystallographic data in CIF or other electronic format see DOI: 10.1039/c9dt00485h



**Scheme 2** Synthesis of **1** by reaction of DIBAC with Na[OCP].



calculated  $^{31}\text{P}$  NMR chemical shift of the  $(\text{iBu})_2\text{Al}-\text{O}-\text{C}\equiv\text{P}$  isomer is  $\delta = -333.0$  ppm, which corresponds well with the experimentally observed one and is significantly different from the calculated  $^{31}\text{P}$  chemical shift of the phosphaketene isomer  $(\text{iBu})_2\text{Al}-\text{P}=\text{C}=\text{O}$  at  $\delta = -353.1$  ppm (DFT: B3LYP/6-311+G(2d,p)).<sup>23</sup> Remarkably, while the latter is not observed in solution, it is predicted to be  $4.4$  kcal mol $^{-1}$  ( $\Delta E$ ) lower in energy than the former which implies **1** to be a kinetic product. Its selective formation may be explained by a preference for oxygen binding of Na[OCP] to  $(\text{iBu})_2\text{AlCl}$  giving the anionic Al–O adduct Na[(iBu)<sub>2</sub>Al(OCP)Cl] as intermediate prior to salt elimination, which is calculated to be  $3.4$  kcal mol $^{-1}$  lower in energy than the corresponding P-coordinated salt Na[(iBu)<sub>2</sub>Al(PCO)Cl].

Complex **1** proved to be persistent in solution for at least two days, however, decomposed to unidentified products upon concentration of the reaction mixture under vacuum. By contrast, employing the five coordinate Schiff-base precursors salen(*t*Bu)AlCl<sup>24</sup> and Salophen(*t*Bu)AlCl<sup>24</sup> in the reaction with Na[OCP] yielded stable aluminum oxyphosphaalkyne complexes **2a** and **2b** (Scheme 3), which could be isolated from toluene in 68% and 40% yield, respectively. Both, the IR OCP stretching frequencies (**2a**:  $\nu = 1692$  cm $^{-1}$ ; **2b**:  $\nu = 1690$  cm $^{-1}$ ), as well as the  $^{31}\text{P}$  NMR chemical shifts (**2a**:  $\delta = -336.8$  ppm in C<sub>6</sub>D<sub>6</sub>; **2b**:  $\delta = -335.2$  ppm in toluene) are comparable to those found for **1**, and similar to the values reported for related Th-,<sup>6</sup> Sc-<sup>8</sup> and Y–O–C≡P<sup>9</sup> complexes ( $\delta^{31}\text{P} = -334.0$ ,  $-343.5$  and  $-346.9$  ppm, respectively), yet significantly shifted from M[OCP] salts (M = Li, Na, K;  $\delta^{31}\text{P} = -384$  to  $-397$  ppm).<sup>1,2</sup>

Light yellow crystals of **2a** were grown from a saturated toluene solution layered with *n*-hexane and used for X-ray diffraction to determine the structure in solid state; a plot is presented in Fig. 1. As expected, the oxygen center of the OCP unit binds to the aluminum center. Compared to Na[OCP] ( $d(\text{O}-\text{C})_{\text{avg.}} = 1.208$  Å;  $d(\text{C}-\text{P})_{\text{avg.}} = 1.575$  Å),<sup>2a</sup> the O1–C1 bond of 1.2538(10) Å is elongated while the C1–P1 bond of 1.5646(9) Å is slightly shortened due to the electron withdrawing aluminium substituent at O1, giving rise to more pronounced single and triple bond character, respectively. This phenomenon is likewise observed in the only other related main group element example of **A** (Scheme 1), that is (N(dipp)CH)<sub>2</sub>B–O–C≡P ( $d(\text{O}-\text{C}) = 1.269(2)$  Å;  $d(\text{C}-\text{P}) = 1.545(2)$  Å).<sup>21</sup>

DFT calculations on the truncated model of **2a** and the corresponding phosphaketene isomer, that is **2a'** and **2a'-I**



Fig. 1 Molecular structure of **2a** in the crystal<sup>25</sup> (ellipsoids are shown at 50% probability; hydrogen atoms are omitted for clarity). Selected bond distances [Å] and angles [°]: C1–P1 1.5646(9), O1–C1 1.2538(10), Al1–O1 1.8206(7), Al1–O2 1.7670(6), Al1–O3 1.7901(6), C1–O1–Al1 131.38(6), O1–C1–P1 177.61(8).



Scheme 4 Synthesis of salen supported [Ga]–P=C=O complex **3**.

(*t*Bu = H; B3LYP/6-311G(2d,p)), were performed to gain insight into their relative energies.<sup>23</sup> In contrast to what was found for the respective isomers of **1**, the O-bound structure is computed to be  $5.0$  kcal mol $^{-1}$  ( $\Delta E$ ) lower in energy than the P-bound one and thereby the thermodynamically favoured product in this case. Presumably, the reverse in order of stability is caused by the more electron deficient O-bound aryloxy groups in **2a** compared to the alkyl substituents in **1**, which make the Al-atom in the former even harder and consequently more oxophilic. When the aluminum center was exchanged for a softer gallium center, the P-coordinated isomer of the type **B** is calculated to be  $8.5$  kcal mol $^{-1}$  lower in energy compared to the corresponding gallium-oxyphosphaalkyne type **A**. Indeed, mixing salen(*t*Bu)GaCl<sup>26</sup> with Na[OCP] in toluene at room temperature gave only phosphaketene **3** which could be isolated in 81% yield (Scheme 4).

The identity of **3** was established in solution by multinuclear NMR spectroscopy and in the solid state by IR spectroscopy and single crystal X-ray diffraction. The  $^{31}\text{P}$  NMR chemical shift was observed at  $\delta = -376.9$  ppm (in THF-*d*<sub>8</sub>) and is in the same range as the ones found for related R–P=C=O species where R = Ph<sub>3</sub>Sn or iPr<sub>3</sub>Si ( $\delta^{31}\text{P} = -378.0$  or  $-370.1$  ppm, respectively), yet upfield to those arising from examples where R = Ph<sub>3</sub>Si or Ph<sub>3</sub>Ge ( $\delta^{31}\text{P} = -340.5$  or  $-344.0$  ppm, respectively).<sup>13d</sup> The asymmetric IR PCO stretching frequency at  $\nu = 1910$  cm $^{-1}$  is characteristic for phosphaketenes (*cf.* Mes\*–P=C=O:<sup>27</sup>  $\nu = 1953$  cm $^{-1}$ ; Ph<sub>3</sub>E–P=C=O (E = Si, Ge, Sn, Pb):<sup>13d</sup>  $\nu = 1923$ – $1962$  cm $^{-1}$ ), as are the crystallographically determined P1–C1 and C1–O1 bond lengths of 1.625(4) Å and 1.189(4) Å, respectively (Fig. 2). These are, however, significantly contracted in comparison to the predicted lengths for P=C and C=O double bonds ( $\sum r_{\text{cov}}(\text{P}=\text{C}) = 1.69$  Å;  $\sum r_{\text{cov}}(\text{C}=\text{O}) = 1.24$  Å).<sup>28</sup>



Scheme 3 Synthesis of salen supported [Al]–O–C≡P complexes **2**.



Fig. 2 Molecular structure of **3** in the crystal<sup>25</sup> (ellipsoids are shown at 50% probability; hydrogen atoms are omitted for clarity). Selected bond distances [Å] and angles [°]: C1–P1 1.625(4), O1–C1 1.189(4), Ga1–P1 2.3761(8), Ga1–O2 1.8748(15), Ga1–O3 1.9073(16), C1–P1–Ga1 88.43(11), O1–C1–P1 177.3(3).

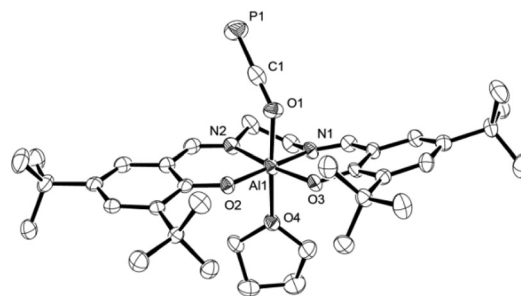
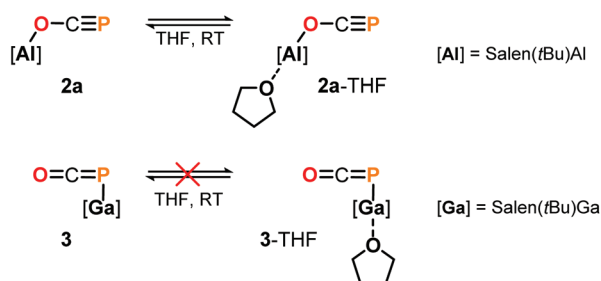


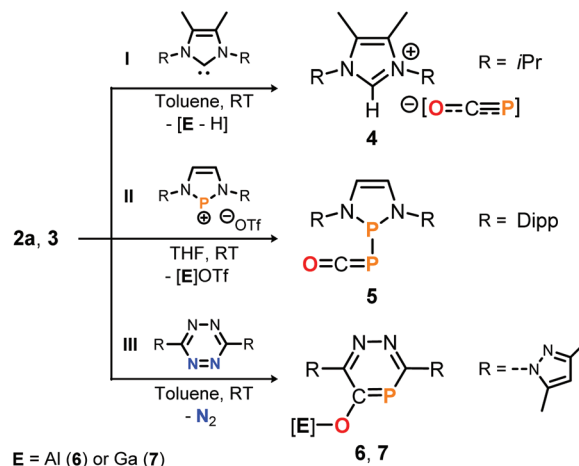
Fig. 3 Molecular structure of **2a-THF** in the crystal<sup>25</sup> (ellipsoids are shown at 50% probability; hydrogen atoms and three toluene molecules are omitted for clarity). Selected bond distances [Å] and angles [°]: C1–P1 1.587(5), C1–O1 1.228(5), Al1–O1 1.920(3), Al1–O2 1.802(3), Al1–O3 1.796(2), Al1–O4 2.040(3), C1–O1–Al1 137.5(2), O1–C1–P1 178.5(3).



Scheme 5 Reactivity of **2a** and **3** in THF.

Some insight into the reactivity of the new adducts **2** and **3** could be acquired by closer inspection of their <sup>31</sup>P NMR spectra in THF-*d*<sub>8</sub> and C<sub>6</sub>D<sub>6</sub>. In case of the Ga–P=C=O compound **3**, spectra in both solvents showed sharp signals at the same chemical shift indicating no significant interaction with the solvents. On the other hand, those recorded of the oxyphosphaalkyne Al adduct **2a** displayed a 17.1 ppm upfield shift and broadening of the <sup>31</sup>P resonance in THF-*d*<sub>8</sub> compared to the one in C<sub>6</sub>D<sub>6</sub> ( $\delta^{31}\text{P} = -353.9$  vs.  $-336.8$  ppm, respectively; see the ESI† for a variable temperature NMR spectroscopy study). These observations may be explained by the reversible coordination of a THF molecule to the Lewis acidic aluminium center in **2a** to form **2a-THF**, which does not occur in case of **3** (Scheme 5). This is corroborated by DFT calculations using the model compounds **2a'** and **3'** (*t*Bu = H),<sup>23</sup> which revealed the formation of **2a'-THF** to be 6.0 kcal mol<sup>-1</sup> downhill in energy ( $\Delta E$ ), while no minimum for **3'-THF** was found. Indeed, crystallization of **2a** from a THF solution layered with toluene/*n*-hexane yielded X-ray quality crystals of **2a-THF**, which allowed elucidation of its solid state structure and revealed a THF bound six-coordinate aluminium core with an elongated Al1–O1 bond (1.920(3) Å) compared to solvent-free complex (Fig. 3; cf. Fig. 1). Consistently, the C1–O1 bond (1.228(5) Å) is found to be slightly shorter and the C1–P1 bond (1.587(5) Å) longer, reflecting a more pronounced delocalization of electron density from O1 into the  $\pi^*$ -orbital of the C1≡P1 bond.

To further explore the Lewis acidic properties of **2a** and **3**, stoichiometric reactions with N-heterocyclic carbene **I** were scrutinized in toluene (Scheme 6, top). Instead of forming an adduct similar to **2a-THF**, however, compound **4** was produced



Scheme 6 Reactivity of **2a** and **3** toward NHC **I**, diazaphosphenium triflate **II** and *s*-tetrazine **III**. OTf = CF<sub>3</sub>SO<sub>3</sub>. [Al] = salen(*t*Bu)Al, [Ga] = salen(*t*Bu)Ga.

in both reactions according to single crystal X-ray diffraction studies for which crystals were used that precipitated directly from the reaction solutions (see the ESI†).<sup>25</sup> These results imply acid–base reactions to have occurred, in which presumably the salen ligands in **2a** and **3** are deprotonated by the NHC and subsequently [OCP]<sup>-</sup> is liberated to form the [NHC–H][OCP] ion pair. Note that **4** is a rare example of a phosphoethynolate anion with a weakly coordinating cation,<sup>15,29</sup> a related example of which could be accessed from the reaction of Na[OCP] with the non-methylated 1,3-diisopropyl imidazolium chloride ( $\delta^{31}\text{P} = -388.0$  ppm; see the ESI† for synthetic details).

The Lewis basic properties of **2a** and **3** were investigated by monitoring their reaction with the diazaphosphenium salt **II** by <sup>31</sup>P NMR spectroscopy (Scheme 6, middle). It was found that the [OCP]<sup>-</sup> ligand in both the Al- and Ga-adduct transfers instantly and irreversibly to the stronger Lewis acid to yield phosphanylphosphaketene **5** quantitatively, as confirmed by comparison of its <sup>31</sup>P NMR resonance signal ( $\delta = 166.1$  and  $-231.8$  ppm, <sup>1</sup>J<sub>P, P</sub> = 253 Hz) with literature values. Compound **5**



was previously prepared from **II** by salt metathesis using Na[OCP] instead.<sup>10f</sup> Finally, the reaction of **2a** with *s*-tetrazine **III** in toluene afforded the *O*-salen(*t*Bu)Al-1,2,4-diazaphosphinine-5-olate **6**, which could be isolated in 46% yield and fully characterized including a structure determination by an X-ray diffraction study using a single crystal (Scheme 6, bottom;  $\delta^{31}\text{P} = 132.0$  ppm; see ESI† for synthetic details<sup>25</sup>). The P-heterocycle is formed through Diels Alder type reactivity of the [Al]-O-C≡P triple bond in **2a** with the tetrazine framework under elimination of dinitrogen. This reaction was recently reported to occur similarly with Na[OCP] as reagent.<sup>30</sup> Remarkably, employing phosphaketene **3** under the same reaction conditions afforded the gallium derivative **7** (75% isolated yield;  $\delta^{31}\text{P} = 133.1$  ppm), suggesting a related [4 + 2]-cycloaddition between the C=P double bond in [Ga]-P=C=O **3** and the tetrazine followed by elimination of N<sub>2</sub> and subsequent 1,3-P,O-migration of the salen gallium fragment.

In summary, the first aluminium and gallium adducts of the phosphoethynolate anion have been isolated and fully characterized. The complexes are supported by bulky salen ligands and reveal a selective binding to O and P, respectively. Preliminary reactivity studies showed that the OCP units in both derivatives are readily liberated from the group 13 element centers by an N-heterocyclic carbene Lewis base, or transferred to a stronger diazaphosphenium Lewis acid. In addition, cycloaddition reactions with *s*-tetrazines under elimination of N<sub>2</sub> were found to give Al- or Ga-complexed 1,2,4-diazaphosphinine-5-olate heterocycles. The studied transformations mimic those previously reported for Na[OCP], which suggests that the Al-O-C≡P and Ga-P=C=O adducts **2** and **3** can serve as neutral and more soluble [OCP]<sup>−</sup> precursors. Moreover, the presence of the bulky Lewis acidic salen(*t*Bu)E centers could facilitate the stabilization and subsequent derivatization of otherwise fleeting phosphoethynolate-derived products.

## Conflicts of interest

There are no conflicts to declare.

## Acknowledgements

This work was supported by the ETH Zürich (project 0-20214-169), and the Lehn Institute of Functional Materials (LIFM), School of Chemistry at the Sun Yat-sen university, the National Natural Science Foundation of China (NSFC) project (21720102007).

## Notes and references

- The first preparation of the phosphoethynolate anion [OCP]<sup>−</sup> was reported by Becker *et al.* in 1992 as Li<sup>+</sup> salt, see: G. Becker, W. Schwarz, N. Seidler and M. Westerhausen, *Z. Anorg. Allg. Chem.*, 1992, **612**, 72–82.
- (a) F. F. Puschmann, D. Stein, D. Heift, C. Hendriksen, Z. A. Gal, H.-F. Grützmacher and H. Grützmacher, *Angew. Chem., Int. Ed.*, 2011, **50**, 8420–8423; (b) D. Heift, Z. Benkő and H. Grützmacher, *Dalton Trans.*, 2014, 831–840; (c) R. Suter, Z. Benkő, M. Bispinghoff and H. Grützmacher, *Angew. Chem., Int. Ed.*, 2017, **56**, 11226–11231; (d) I. Krummenacher and C. C. Cummins, *Polyhedron*, 2012, **32**, 10–13; (e) A. R. Jupp and J. M. Goicoechea, *Angew. Chem., Int. Ed.*, 2013, **52**, 10064–10067.
- For reviews, see: (a) H. Grützmacher and J. Goicoechea, *Angew. Chem., Int. Ed.*, 2018, **57**, 16968–16994; (b) L. Weber, *Eur. J. Inorg. Chem.*, 2018, 2175–2227.
- M. Westerhausen, S. Schneiderbauer, H. Piotrowski, M. Suter and H. Nöth, *J. Organomet. Chem.*, 2002, **643–644**, 189–193.
- R. J. Gilliard, D. Heift, Z. Benkő, J. M. Keiser, A. L. Rheingold, H. Grützmacher and J. D. Protasiewicz, *Dalton Trans.*, 2018, 666–669.
- C. Camp, N. Settineri, J. Lefèvre, A. R. Jupp, J. M. Goicoechea, L. Maron and J. Arnold, *Chem. Sci.*, 2015, **6**, 6379–6384.
- C. J. Hoerger, F. W. Heinemann, E. Louyriac, L. Maron, H. Grützmacher and K. Meyer, *Organometallics*, 2017, **36**, 4351–4354.
- L. N. Grant, B. Pinter, B. C. Manor, H. Grützmacher and D. J. Mindiola, *Angew. Chem., Int. Ed.*, 2018, **57**, 1049–1052.
- S. Bestgen, Q. Chen, N. H. Rees and J. M. Goicoechea, *Dalton Trans.*, 2018, 13016–13024.
- (a) M. M. Hansmann, D. A. Ruiz, L. Liu, R. Jazzar and G. Bertrand, *Chem. Sci.*, 2017, **8**, 3720–3725; (b) L. Liu, D. A. Ruiz, D. Munz and G. Bertrand, *Chem*, 2016, **1**, 147–153; (c) Z. Li, X. Chen, Z. Benkő, L. Liu, D. A. Ruiz, J. L. Peltier, G. Bertrand, C.-Y. Su and H. Grützmacher, *Angew. Chem., Int. Ed.*, 2016, **55**, 6018–6022; (d) M. M. Hansmann, R. Jazzar and G. Bertrand, *J. Am. Chem. Soc.*, 2016, **138**, 8356–8359; (e) M. M. Hansmann and G. Bertrand, *J. Am. Chem. Soc.*, 2016, **138**, 15885–15888; (f) Z. Li, X. Chen, M. Bergeler, M. Reiher, C.-Y. Su and H. Grützmacher, *Dalton Trans.*, 2015, 6431–6438.
- T. Krachko, A. W. Ehlers, M. Nieger, M. Lutz and J. C. Sloatweg, *Angew. Chem., Int. Ed.*, 2018, **57**, 1683–1687.
- (a) A. Hinz and J. M. Goicoechea, *Chem. – Eur. J.*, 2018, **24**, 7358–7363; (b) Y. Xiong, S. Yao, T. Szilvási, E. Ballester-Martínez, H. Grützmacher and M. Driess, *Angew. Chem., Int. Ed.*, 2017, **56**, 4333–4336; (c) S. Yao, Y. Xiong, T. Szilvási, H. Grützmacher and M. Driess, *Angew. Chem., Int. Ed.*, 2016, **55**, 4781–4785; (d) N. Del Rio, A. Baceiredo, N. Saffon-Merceron, D. Hashizume, D. Lutters, T. Müller and T. Kato, *Angew. Chem., Int. Ed.*, 2016, **55**, 4753–4758; (e) Y. Wu, L. Liu, J. Su, J. Zhu, Z. Ji and Y. Zhao, *Organometallics*, 2016, **35**, 1593–1596.
- (a) A. Hinz and J. M. Goicoechea, *Dalton Trans.*, 2018, 8879–8883; (b) Z. Li, X. Chen, Y. Li, C.-Y. Su and H. Grützmacher, *Chem. Commun.*, 2016, **52**, 11343–11346; (c) D. Heift, Z. Benkő and H. Grützmacher, *Chem. – Eur. J.*,



- 2014, **20**, 11326–11330; (d) D. Heift, Z. Benkő and H. Grützmacher, *Dalton Trans.*, 2014, 5920–5928.
- 14 S. Alidori, D. Heift, G. Santiso-Quinones, Z. Benkő, H. Grützmacher, M. Caporali, L. Gonsalvi, A. Rossin and M. Peruzzini, *Chem. – Eur. J.*, 2012, **18**, 14805–14811.
- 15 L. Liu, D. A. Ruiz, F. Dahcheh, G. Bertrand, R. Suter, A. M. Tondreau and H. Grützmacher, *Chem. Sci.*, 2016, **7**, 2335–2341.
- 16 L. N. Grant, B. Pinter, B. C. Manor, R. Suter, H. Grützmacher and D. J. Mindiola, *Chem. – Eur. J.*, 2017, **23**, 6272–6276.
- 17 Protonation occurs likewise at the P-atom, see: A. Hinz, R. Labbow, C. Rennick, A. Schulz and J. M. Goicoechea, *Angew. Chem., Int. Ed.*, 2017, **56**, 3911–3915.
- 18 Carbene-coordinated Ni(C<sub>5</sub>H<sub>5</sub>), Ag(OSO<sub>2</sub>CF<sub>3</sub>) and Cu(OtBu) compounds were likewise found to engage in a salt metathesis reaction with Na[OCP], giving pi-coordinated phosphaketene complexes. See: (a) G. Hierlmeier, A. Hinz, R. Wolf and J. M. Goicoechea, *Angew. Chem., Int. Ed.*, 2018, **57**, 431–436; (b) M. M. D. Roy, M. J. Ferguson, R. McDonald and E. Rivard, *Chem. Commun.*, 2018, **54**, 483–486; (c) Ref. 15.
- 19 K. Nakajima, W. Liang and Y. Nishibayashi, *Org. Lett.*, 2016, **18**, 5006–5009.
- 20 R. Suter, Y. Mei, M. Baker, Z. Benkő, Z. Li and H. Grützmacher, *Angew. Chem., Int. Ed.*, 2017, **56**, 1356–1360.
- 21 D. W. N. Wilson, A. Hinz and J. M. Goicoechea, *Angew. Chem., Int. Ed.*, 2018, **57**, 2188–2193.
- 22 The coordination chemistry of Na[OCP] toward pentaphenylborole and arylboranes was also studied and revealed the formation of P-heterocycles, see: (a) K. M. Szkop, A. R. Jupp, R. Suter, H. Grützmacher and D. W. Stephan, *Angew. Chem., Int. Ed.*, 2017, **56**, 14174–14177; (b) Y. Li, R. K. Siwatch, T. Mondal, Y. Li, R. Ganguly, D. Koley and C.-W. So, *Inorg. Chem.*, 2017, **56**, 4112–4120.
- 23 See the ESI† for further details.
- 24 Salen(*t*Bu) = *N,N'*-ethylenebis(3,5-di-*tert*-butylsalicylideneimine); Salophen(*t*Bu) = *N,N'*-benzenylidenebis(3,5-di-*tert*-butyl salicylideneamine). The [Al]Cl precursors were prepared according to literature procedures, see: D. Rutherford and D. A. Atwood, *Organometallics*, 1996, **15**, 4417–4422.
- 25 CCDC 1860668 (**2a**), 1860669 (**2a**-THF), 1860673 (**3**), 1860732 (**6**) and 1860759 (**4**)† contain the supplementary crystallographic data for this paper.
- 26 The [Ga]Cl precursor was prepared according to a literature procedure: D. J. Darensbourg and D. R. Billodeaux, *C. R. Chim.*, 2004, **7**, 755–761.
- 27 R. Appel and W. Paulen, *Angew. Chem.*, 1983, **95**, 807–808. Mes\* = 2,4,6-tri-*tert*-butylphenyl.
- 28 P. Pykkö and M. Atsumi, *Chem. – Eur. J.*, 2009, **15**, 12770–12779.
- 29 M. Jost, L. H. Finger, J. Sundermeyer and C. von Hänisch, *Chem. Commun.*, 2016, **52**, 11646–11648.
- 30 (a) A. V. Polezhaev, D. M. Beagan, A. C. Cabelof, C.-H. Chen and K. G. Caulton, *Dalton Trans.*, 2018, 5938–5942; (b) M. M. Hansmann, *Chem. – Eur. J.*, 2018, **24**, 11573–11577.

